

PACS numbers: 42.55.Wd; 42.60.Da; 42.60.Fc
DOI: 10.1070/QE2010v040n02ABEH014225

High-index-ring three-layer fibres for mode-locked sub-1.3 μm fibre lasers

A.S. Belanov, S.V. Tsvetkov

***Abstract*. This paper addresses issues pertaining to the propagation of ultrashort pulses in the cavities of mode-locked sub-1.3 μm fibre lasers. We demonstrate that multimode high-index-ring three-layer optical fibres operating on a single higher order HE_{1m} mode are an effective approach to dispersion compensation. We present optimal parameters of the refractive-index profile in such fibres, which ensure zero first- and second-order chromatic dispersion coefficients at 1.06 μm for the HE_{12} and HE_{13} modes, and analyse their dispersion and power parameters.**

Keywords: *multimode high-index-ring three-layer optical fibre, fibre lasers, femtosecond pulses, higher order modes, chromatic dispersion, effective mode area, mode energy*.

1. Introduction

Mode-locked fibre lasers use optical fibres doped with erbium, ytterbium, neodymium, bismuth and other ions [1 – 3]. The broad gain bands of these elements enable the generation of ultrashort (femtosecond) pulses with a very high repetition rate (above 1 THz). The pulse energy, pulse shape quality and the peak power of fibre lasers are however severely limited by the chromatic dispersion and nonlinearity of the fibre.

The dispersion problem arises when a pulse has to travel a large distance through fibre in a laser cavity, with the largest contribution to the pulse shape distortion made by chromatic dispersion. In view of this, fibre lasers must use zero-dispersion or anomalous-dispersion (compensating) fibres. Erbium fibre lasers operate in the range 1.5 – 1.6 μm, where good chromatic dispersion compensation is ensured by single-mode fibres. Ytterbium-, neodymium- and bismuth-doped fibre lasers emit in the range 0.9 – 1.2 μm. At these wavelengths, all single-mode fibres have normal chromatic dispersion, which, in addition, rapidly increases in magnitude with decreasing wavelength. To compensate for the normal chromatic dispersion in such lasers, use is typically made of special fibre Bragg gratings or photonic-crystal fibres [4 – 7, 12].

A.S. Belanov, S.V. Tsvetkov Moscow State University of Instrument Engineering and Informatics, ul. Stromynka 20, 107996 Moscow, Russia; e-mail: it3@mgupi.ru

Received 1 October 2009
Kvantovaya Elektronika **40** (2) 160 – 162 (2010)
Translated by O.M. Tsarev

The generation of the shortest possible pulses requires both first- and second-order chromatic dispersion compensation. The first-order chromatic dispersion coefficient is given by

$$S_1 = \frac{1}{c}\frac{\mathrm{d}n_{\mathrm{gr}}}{\mathrm{d}\lambda} = -\frac{\lambda}{c}\frac{\mathrm{d}^2 n_{\mathrm{eff}}}{\mathrm{d}\lambda^2} \quad (1)$$

(measured in ps km^{-1} nm^{-1}), and the second-order chromatic dispersion coefficient is

$$S_2 = \frac{\mathrm{d}S_1}{\mathrm{d}\lambda} = -\frac{1}{c}\left(\frac{\mathrm{d}^2 n_{\mathrm{eff}}}{\mathrm{d}\lambda^2} + \lambda\frac{\mathrm{d}^3 n_{\mathrm{eff}}}{\mathrm{d}\lambda^3}\right) \quad (2)$$

(measured in ps km^{-1} nm^{-2}), where $n_{\mathrm{gr}} = n_{\mathrm{eff}} - \lambda\times(\mathrm{d}n_{\mathrm{eff}}/\mathrm{d}\lambda)$ is the group refractive index of the fibre mode; n_{eff} is the effective refractive index of the mode; λ is the wavelength of the incident light in vacuum; and c is the speed of light in vacuum.

Problems arising from the nonlinearity of the fibre core material are usually resolved by increasing the effective mode area and optimising the transverse intensity profile of the mode. Because the effective mode area in single-mode fibres is small, use is made, when necessary, of purpose-designed photonic-crystal fibres [8].

In recent years, to achieve the desired dispersion and power performance, considerable effort has been focused on the study of multimode fibres [9 – 11], which can be made to operate on a single higher order mode using, e.g., long-period Bragg gratings [12]. Such modes are HE_{1m} (replaced by LP_{0m} in approximate calculations) of radial order $m > 1$.

This paper examines three-layer multimode fibres which, when operating on a single higher order HE_{1m} mode, have zero first- and second-order chromatic dispersion in the spectral region of ytterbium and neodymium fibre lasers. All our calculations rely on a rigorous theory of guided modes in cylindrical multilayer fibres [13, 14].

2. Structure of high-index-ring fibres

A model three-layer high-index-ring fibre consists of a core, first cladding and second cladding, with refractive indices n_1, n_2 and n_3, respectively (Fig. 1): $n_2 > n_1 > n_3$. The refractive-index profile of the fibre is radially symmetric.

Consider two high-index-ring fibres, F1 and F2, with parameters listed in Table 1. In both fibres, the core and first cladding are doped with germania, GeO_2, to concentrations c_1 and c_2, respectively. The second cladding consists of pure silica: $c_3 = 0$. The refractive indices n_1, n_2 and n_3 at 1.06 μm

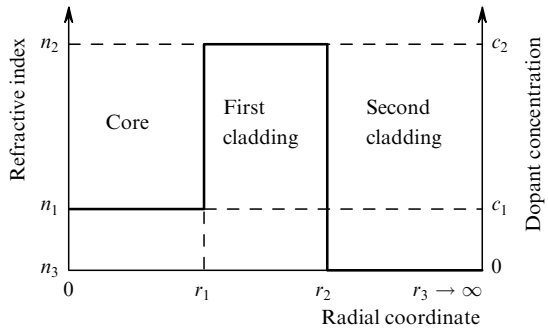

Figure 1. Refractive-index (GeO_2 concentration) profile of a high-index-ring three-layer fibre.

were evaluated by the Sellmeier formula [15]. The thicknesses of the layers in the fibres are determined by their outer radii r_1, r_2 and r_3, with the radius of the second cladding being infinitely large.

Table 1. Parameters of the fibres.

Fibre	n_1 (c_1/mol %)	n_2 (c_2/mol %)	n_3 (c_3/mol %)	r_1/μm	r_2/μm
F1	1.46035 (7.17)	1.47781 (19)	1.44968 (0)	3.311	4.3
F2	1.45157 (1.26)	1.45713 (5)	1.44968 (0)	8.6685	13.6835

3. Dispersion characteristics of the high-index-ring fibres

To achieve the above dispersion characteristics in F1 and F2, namely, zero first- and second-order chromatic dispersion coefficients at 1.06 μm, the fibres must support only the HE_{12} and HE_{32} modes, respectively. The use of lower order HE_{1m} modes does not give the desired result. At 1.06 μm, we obtain $S_1 = -76.6$ ps km^{-1}nm^{-1} for the HE_{11} mode of F1, $S_1 = -32.3$ ps km^{-1}nm^{-1} for the HE_{11} mode of F2 and $S_1 = -72$ ps km^{-1}nm^{-1} for its HE_{12} mode.

Figure 2 plots S_1 against wavelength for the HE_{12} and HE_{13} modes of F1 and F2. The first- and second-order dispersion compensation regions are near $\lambda = 1.06$ μm and correspond to the maxima in the dispersion curves. By varying the index profile, the maxima can be shifted to either side along both axes: increasing the refractive indices (GeO_2 content) of the layers and the fibre radius shifts the dispersion maximum to the anomalous dispersion region and to longer wavelengths. It should, however, be kept in mind that increasing the refractive indices reduces the effective mode area and that raising the GeO_2 concentration increases the optical loss in the material [16] and its nonlinearity [17].

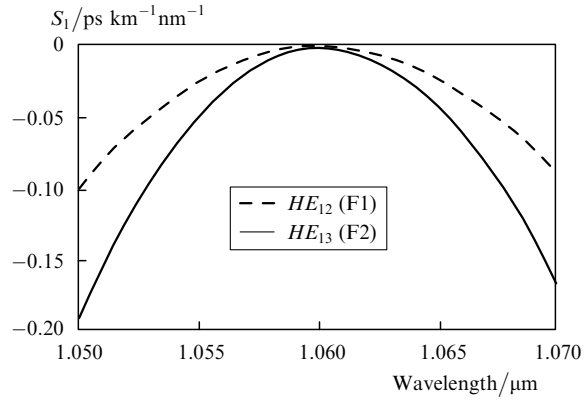

Figure 2. First-order chromatic dispersion coefficient vs. wavelength for the HE_{12} and HE_{13} modes of F1 and F2.

4. Power parameters of the high-index-ring fibres

Power parameters such as the effective mode area, transverse intensity profile of the fibre and the relationship between the powers deposited in its layers are clearly represented by the radial distribution of the longitudinal component of the mode energy flux density vector:

$$S_z = \frac{1}{2}\,\mathrm{Re}\left(E_r H_\varphi^* - E_\varphi H_r^*\right), \tag{3}$$

where E_r and E_φ are the radial and azimuthal components of the electric field vector of the mode, and H_r and H_φ are those of its magnetic field vector.

Figure 3 shows two normalised radial distributions of the energy flux density for the HE_{12} and HE_{13} modes of F1 and F2, respectively. As seen, in both fibres most of the power will propagate through the core. The fractions of the power in the core, first cladding and second cladding are, respectively, 78.6 %, 11.4 % and 10.0 % for F1 and 70.9 %, 19.0 % and 10.1 % for F2.

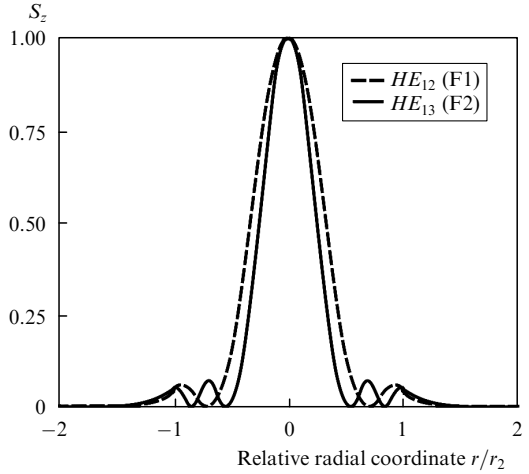

Figure 3. Normalised radial distributions of the energy flux density for the HE_{12} and HE_{13} modes of F1 and F2.

The effective HE_{12} and HE_{13} mode areas evaluated as

$$A_{\mathrm{eff}} = \left[\int_0^{2\pi}\int_0^{\infty} |S_z(r,\varphi)|\,r\mathrm{d}r\mathrm{d}\varphi\right]^2 \Big/ \int_0^{2\pi}\int_0^{\infty} |S_z(r,\varphi)|^2\,r\mathrm{d}r\mathrm{d}\varphi \tag{4}$$

are 21.7 μm^2 in F1 and 159.4 μm^2 in F2. An important point is that most of the power of both the HE_{12} and HE_{13} modes will be concentrated in the lightly doped central region, which offers lower nonlinearity and low losses [16, 17].

5. Conclusions

The creation of all-fibre lasers ensuring distortion-free transmission of ultrashort, very high power pulses at ~ 1 μm is a challenging problem. In this context, an important aspect of the present results is that high-index-ring fibres operating on a single HE_{1m} ($m > 1$) mode can at least provide the dispersion characteristics necessary for this.

The proposed index profiles (F1 and F2) ensure zero first- and second-order dispersion coefficients at 1.06 μm for the HE_{12} and HE_{13} modes, respectively, but only F2 has a sufficiently large effective HE_{13} mode area (about 160 μm^2) and low dopant concentration in the core (1.26 mol % GeO_2). In conjunction with the radial mode energy distribution in this fibre, this ensures an optical loss coefficient close to that of pure fused silica and allows F2 to be used for elevated-power pulse transmission.

References

1. Barnes W. L. et al. *J. Lightwave Technol.*, **7**, 1461 (1989).
2. Krennrich D. et al. *Appl. Phys. B*, **92**, 165 (2008).
3. Dianov E.M., Dvoyrin V.V., Mashinskii V.M., Umnikov A.A., Yashkov M.V., Gur'yanov A.N. *Kvantovaya Elektron.*, **35**, 1083 (2005) [*Quantum Electron.*, **35**, 1083 (2005)].
4. Turchinovich D.et al. *Opt. Express*, **16**, 14004 (2008).
5. Collings B.C. et al. *IEEE J. Sel. Top. Quantum Electron.*, **3**, 1065 (1997).
6. Fermann M. E. et al. *Opt. Lett.*, **20**, 172 (1995).
7. Krylov I.A., Kryukov P.G., Dianov E.M., Okhotnikov O.G., Guina M. *Kvantovaya Elektron.*, **39**, 21 (2009) [*Quantum Electron.*, **39**, 21 (2009)].
8. Lim H., Ilday F.Ö., Wise F.W. *Opt. Express*, **25**, 1497 (2002).
9. Grüner-Nielsen L., Ramachandran S., Jespersen K., Ghalmi S., Garmund M., Pálsdóttir B. *Proc. SPIE Int. Soc. Opt. Eng.*, **6873**, 68730Q (2008).
10. Farrow R., Hadley G., Kliner D., Koplow J. *Proc. SPIE Int. Soc. Opt. Eng.*, **6453**, 64531C (2007).
11. Belanov A.S., Dianov E.M., Sysolyatin A.A., Kharitonova K.Yu., Tsvetkov S.V. *Kvantovaya Elektron.*, **39**, 197 (2009) [*Quantum Electron.*, **39**, 197 (2009)].
12. Kashyap R. *Fiber Bragg Gratings* (London: Acad. Press, 1999).
13. Belanov A.S. *Doct. Diss.* (Moscow: P.N. Lebedev Physics Inst., 1981).
14. Snyder A.W., Love J.D. *Optical Waveguide Theory* (London: Chapman and Hall, 1983; Moscow: Radio i Svyaz', 1987) p. 656.
15. Fleming J.W. *Appl. Opt.*, **24**, 4486 (1984).
16. Likhachev M.E., Bubnov M.M., Semenov S.L., Shvetsov V.V., Khopin V.F., Gur'yanov A.N., Dianov E.M. *Kvantovaya Elektron.*, **33**, 633 (2003) [*Quantum Electron.*, **33**, 633 (2003)].
17. Agrawal G.P. *Nonlinear Fiber Optics* (San Diego: Academic, 2001; Moscow: Mir, 1996).